Proceedings of the Institute of Acoustics

UNDERWATER SOUND PROPAGATION FROM A SOURCE CLOSE TO A WAVY FREE SURFACE

Y He Dept. Mechanical Engineering, University College London
T A Smith Dept. Mechanical Engineering, University College London

1 INTRODUCTION

Understanding how underwater noise propagates from a source close to a free surface has a number of important applications, including for propagation loss calculations for acoustic trials of specific vessels, soundscape modelling, and underwater communication and sonar modelling. For a source close to a flat free surface, the Lloyd's Mirror effect dominates, leading to a dipolar directivity pattern and strong attenuation of low frequency noise close to the free surface. This effect is well understood and has been offered as an explanation for why whales and other mammals sometimes fail to detect approaching ships[1]. The effect becomes more pronounced as the source moves closer to the free surface, and so is particularly prominent for small vessels with shallow draughts[2,3]. However, few studies have considered how this is altered by free surface waves. Whilst acoustic trial guidelines state that trials should be carried out in relatively benign sea states, vessels will still operate outside of these and so it is of interest to understand what effect this has on the radiated noise levels for a vessel. Furthermore, small vessels can experience significant motions even in relatively calm waters, and so being able to quantify the effect of this on radiated noise levels is also useful here.

Current studies concerning low-frequency (≤ 1kHz) noise propagation generally treat the free surface as a flat reflective boundary. For example, Picciulin et al[3] calculated the transmission loss of noise in shallow water using the Parabolic Equation (PE) and Ray theory to numerically model propagation losses from small vessels. Studies that do account for a non-flat free surface tend to focus on higher frequencies, with applications in sonar modelling and underwater communications. Jones et al[4,5] applied time-domain ray tracing and frequency-domain PE separately to determine the scattering at mid frequencies (above 1kHz). However, sources for both cases are placed at 18m depth, where the Lloyd's mirror effect is reduced. Rosenberg et al[6] introduced a wind sea spectra for modelling a realistic rough surface when solving the Parabolic Equation to understand its effect on acoustic communications, where source is placed deep at 46m of a 47.5m depth sea. As with many other similar works, the frequencies considered here were higher than the low frequency tonal noise associated with marine vessels and the sources are not close to the free surface. One study that does consider a source close to a wavy free surface is that of Tindle & Dean[7] who use wavefront modelling to show that free surface waves create acoustic focusing and defocusing.

In this work, the Helmholtz equation is used to provide insights into how free surface waves alter the directivity and radiated levels of low frequency noise from a source close to the free surface. The location of the source relative to a wave crest or trough is considered alongside the free surface wavelength. Shallow water effects are also considered. Results are compared to those with a flat free surface to enable us to investigate how the wavy surface alters the Lloyd's Mirror effect.

2 METHODS

2.1 Governing equations and simulation setup

Many studies into underwater noise propagation utilise the parabolic equation due to its efficiency. However, in this work we have adopted the Helmholtz equation, from which the parabolic equation is derived. This is more complete, and because we are only concerned with low frequency noise propagating over relatively short distances, it is not prohibitively expensive. The approach for this study is to numerically solve the Helmholtz Equation using the Finite Element Method with a Quadratic Lagrange interpolating polynomial. The inhomogeneous Helmholtz Equation applied here approximates the standard wave equation yielded from isentropic wave equations for pressure wave that independent of time in lossless medium:

$$\frac{\partial^2 p}{\partial t^2} = c^2 \boldsymbol{\nabla}^2 p \tag{1}$$

As for the time-dependent pressure, the time derivative is replaced by $i\omega$:

$$p(\mathbf{x}, t) = p(\mathbf{x}) e^{i\omega t} \tag{2}$$

Assuming the same harmonic time dependence for both monopole and dipole source terms, the inhomogeneous Helmholtz Equation is:

$$\boldsymbol{\nabla} \cdot (-\frac{1}{\rho_c})(\boldsymbol{\nabla}_p - \mathbf{q}_d) - \frac{\omega^2 p}{\rho_c c_c^2} = Q_m \tag{3}$$

2D-Axisymmetric model is applied while solving HE using 2D×N, reduce the 3D problem of $p(r, z, \phi)$ to multiple 2D problems of $p(r, z)e^{-im\phi}$ (where m denotes the azimuthal mode number), reserves the azimuth angle dependency but greatly saves computational cost. As the result, HE becomes:

$$\boldsymbol{\nabla} \cdot (-\frac{1}{\rho_c})(\boldsymbol{\nabla}_p - \mathbf{q}_d) - \frac{k_{eq}^2 p}{\rho_c} = Q_m \tag{4}$$

Where $k_{eq}^2 = (\frac{\omega}{c_c})^2 - k_m^2,\ k_m = \frac{m}{r}$

In this work we consider both deep and shallow water. Both cases contain water and air domains, with the deep water domain having 300m water and the shallow water domain is 50m deep. In the case of the deep water simulations, a perfectly matched layer is used at the bottom and right-hand-side boundaries, as well as at the top of the domain. For the shallow water case, an additional region is used to model the seabed as a homogeneous substrate and a perfectly matched layer is used at the bottom of this. The left boundary is a symmetry, and a 0.1m diameter monopole source is located below the free surface on the left-hand-side. Source frequencies of 125Hz and 500Hz are considered. The free surface wave parameters have been chosen to reflect a moderate sea state at two wave lengths, commensurate with upper sea state 4 / lower sea state 5. 3 source depths are chosen, with positions under the wave crest, the wave trough, and under a flat free surface. The parameters are listed in the table 1.

2.2 Verification

Verification of the numerical approach is done via the grid sensitivity analysis and a comparison with the ECHO approach[9]. Figure 1 shows the acoustic field consisting of a source in the top left corner below the crest of a wavy free surface. 2, 5, 15 and 30 grids per wavelength at are considered, and it can be seen that the results for 15 and 30 points per wavelength are almost identical. The ECHO certification

Parameter	Value	Description
a_w	1.25 m	Free surface wave amplitude
c_a	343 m/s	Sound speed in air
c_b	1700 m/s	Sound speed in seabed (soft)
c_w	1500 m/s	Sound speed in water
d_{dw}	300 m	Deep Water depth
d_s	0.1 m, 0.5 m, 1 m	Source depth
d_{sw}	50 m	Shallow water depth
f_N	125 Hz, 500 Hz	URN frequency
p_s	56.23 Pa[3]	URN source pressure
λ_N	12 m, 3 m	URN wavelength
λ_w	28m, 56m	Free surface wavelength
ρ_b	1200 kg/m^3 [8]	Density of seabed (soft)
ρ_w	1025kg/m^3 [8]	Density of seawater

Table 1: Table of parameters

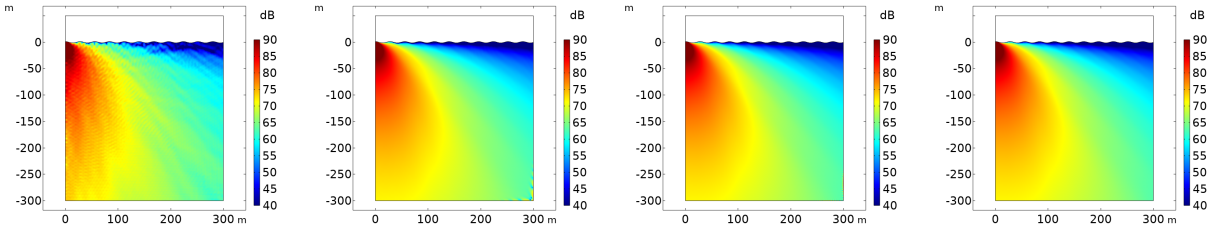

(a) ***(b)*** ***(c)*** ***(d)***

Figure 1: Grid sensitivity analysis, graphs show number of grids per wavelength at 125Hz under a wavy surface (a) 2 grids; (b) 5 grids; (c) 15 grids; (d) 30 grids

alignment project provides an analytical method for computing propagation losses at arbitrary slant angles including the Lloyd's mirror effect. In this approach, the source level is:

$$L_S = L_{RN} - \Delta L_{ECA} + \Delta L_\alpha \tag{5}$$

$$\Delta L_{ECA} = 10 log_{10} \gamma \; dB \tag{6}$$

Where γ is conversion factor of dipole to monopole.

$$\gamma(\theta) = 2 - \frac{sin(2\pi T f_2) - sin(2\pi T f_1)}{\pi T (f_2 - f_1)} \tag{7}$$

Where f_1 and f_2 are lower and upper frequencies, and $T = 2dsin(\theta)/c_w$. d denotes the source depth and c_w is the speed of sound in water. ΔL_α an is absorption factor, accounts for the sound energy loss from simplified Francois-Garrison formula. However, the losses below 1kHz is smaller than 0.01 dB/km, thus neglected[10]. Figure 2 presents a comparison of the ECHO method and the simulations for a source at 500Hz below a flat free surface at a slant range of 118m and slant angles of $10° \leq \theta \leq 60°$. The difference is less than 1.95dB across all angles, providing further confidence in the numerical approach.

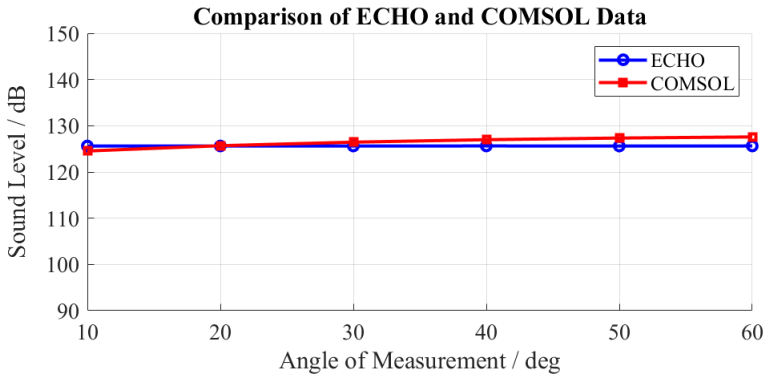

Figure 2: Comparison between simulation result and ECHO calculation of source level across 118m at 500Hz, grazing angle measured from 10 to 60 degrees

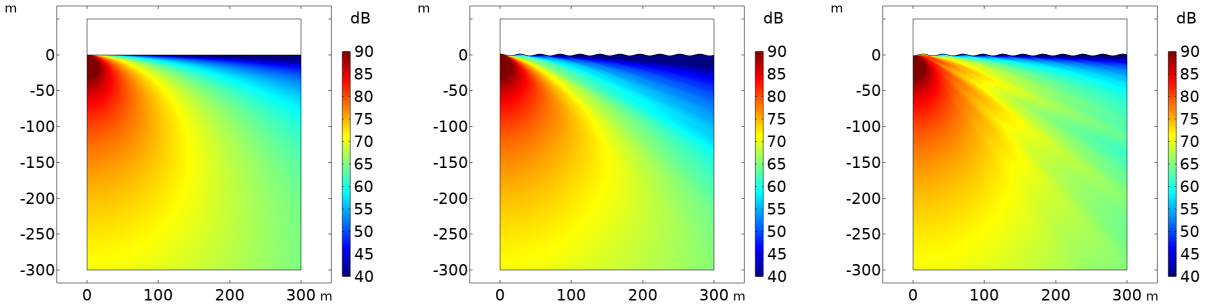

(a) ***(b)*** ***(c)***

Figure 3: Sound Level of below (a) flat free surface; (b) wave crest; (c) wave trough where $d_s = 0.1m$***,*** $\lambda_w = 28m$***,*** $f_N = 500Hz$

3 RESULTS

3.1 Overview of results

Figure 3 shows the acoustic field produced by a source located 0.1 m below a flat free surface, a wave crest, and wave trough in a deep water. While the flat surface reveals the characteristic dipole pattern from the Lloyd's mirror effect, the wavy free surface alters this effect for both cases under different positions of the free surface wave. When the source is below a wave crest, it can be seen that the concave curvature of surface wave refocuses the noise, leading to a reduction close to the free surface compared with a flat surface. The sound level below the source is largely unchanged. This contrasts with the case of the source below a wave trough, which focuses the sound towards the free surface. This case also leads to a more spatially varying field, which is clearly visible in figure 3c.

Figure 4 takes a closer look at the sound level near the free surface. The most obvious local effect is the existence of acoustic shadow regions under the wave for the case of a source under a wave crest. These regions have sound levels significantly lower than those for the flat free surface, both close to the source and further away. For instance, at the second wave from the source (42m – 70m), there exists a 1m deep region where the sound level is below 20 dB, with the depth of this region increasing to 4m for the wave between 126m and 154m. For the case of the source under a trough, these shadow regions are

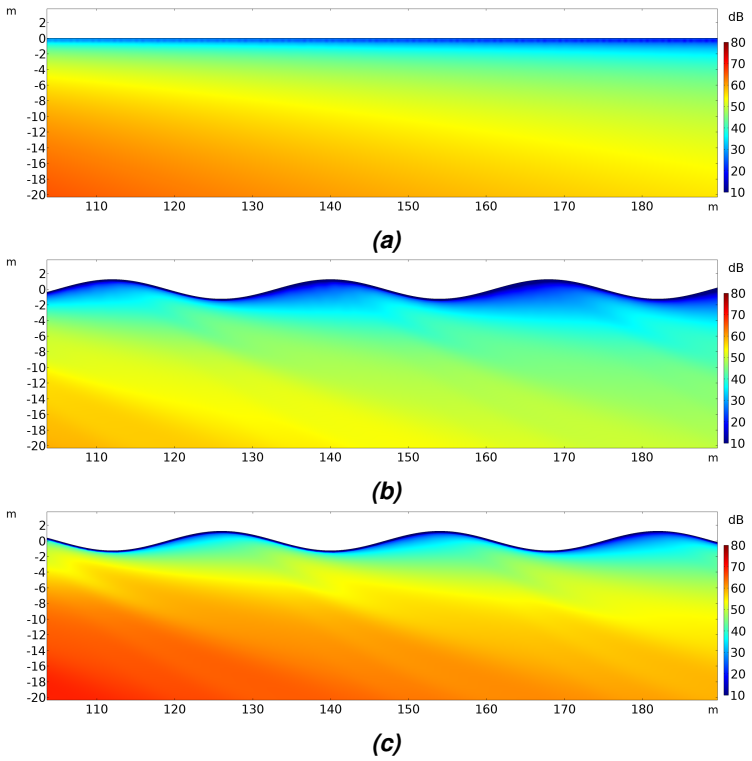

Figure 4: Zoomed in result of SL for source below a (a) flat; (b) wave crest; (c) wave trough at $d_s = 0.1m$**,** $\lambda_w = 28m$**,** $f_N = 500Hz$

still present but significantly smaller.

3.2 Influence of free surface wavelength and acoustic frequency

To understand the impact of free surface wavelength to the noise propagation, the sound level differences (wavy compared with flat free surface) for the whole domain are computed. Figure 5 presents the sound level difference at two frequencies and two free surface wavelengths where the source is 0.1m under a wave crest and under a flat surface. Although four plots are at different surface wavelengths and acoustic frequencies, all of them show a distinct diagonal line that extends the width of the domain. Above this line, the sound level is lower and this region of reduced noise increases in depth going further away from the source. Reductions in sound level of up to 7dB are observed, with the effect being stronger closer to the free surface. Below the diagonal line, the change is sound level is very small. Comparing 5a to 5c and 5b to 5d, it can be seen that lower frequencies result in a steeper slope and a larger area of lower sound. However, the sound level is most reduced at the higher frequency for regions close to the free surface. As one might expect, the larger free surface wavelength reduces the effect of the free surface and it would of interest to consider a broader range of wavelengths to provide a more complete description of how this alters the acoustic field.

Depending on whether the source is below a wave crest or a wave trough, the sound level close to the free surface can either decrease or increase. This is shown in figure 6 for a 500 Hz source located 0.5m below a free surface. Again, differences in sound level compared to a flat free surface are shown. As with the previous results, the source below a wave crest reduces the sound close to the free surface.

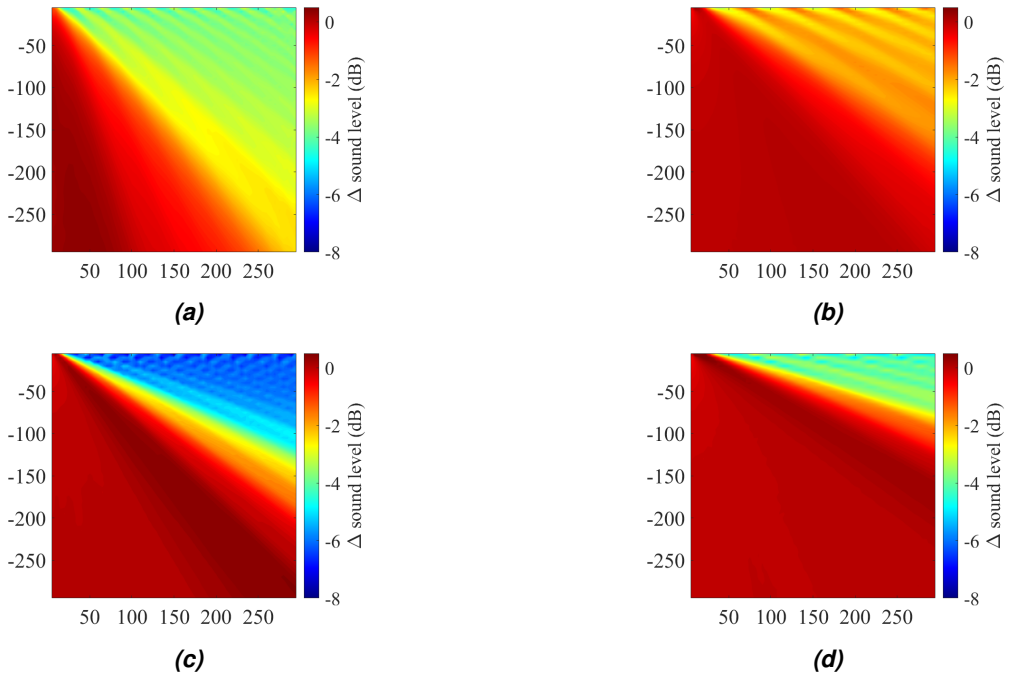

Figure 5: SL difference plot $SL_{crest} - SL_{flat}$ ***at (a)*** $f_N = 125Hz, \lambda_w = 28m$***; (b)*** $f_N = 125Hz, \lambda_w = 56m$***; (c)*** $f_N = 500Hz, \lambda_w = 28m$***; (d)*** $f_N = 500Hz, \lambda_w = 56m$

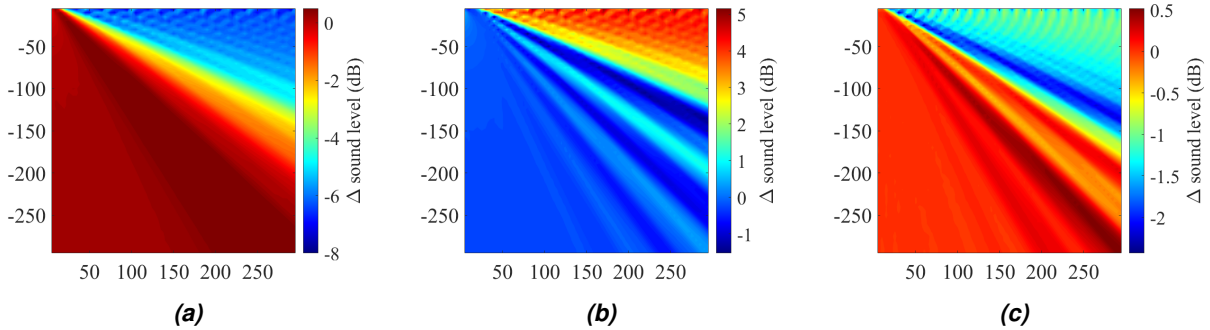

Figure 6: Sound level difference plot of (a) $SL_{crest} - SL_{flat}$***; (b)*** $SL_{trough} - SL_{flat}$***; (c)*** $0.5(SL_{crest} + SL_{trough}) - SL_{flat}$ ***at*** $f_N = 500Hz$ ***and*** $\lambda_w = 28m$

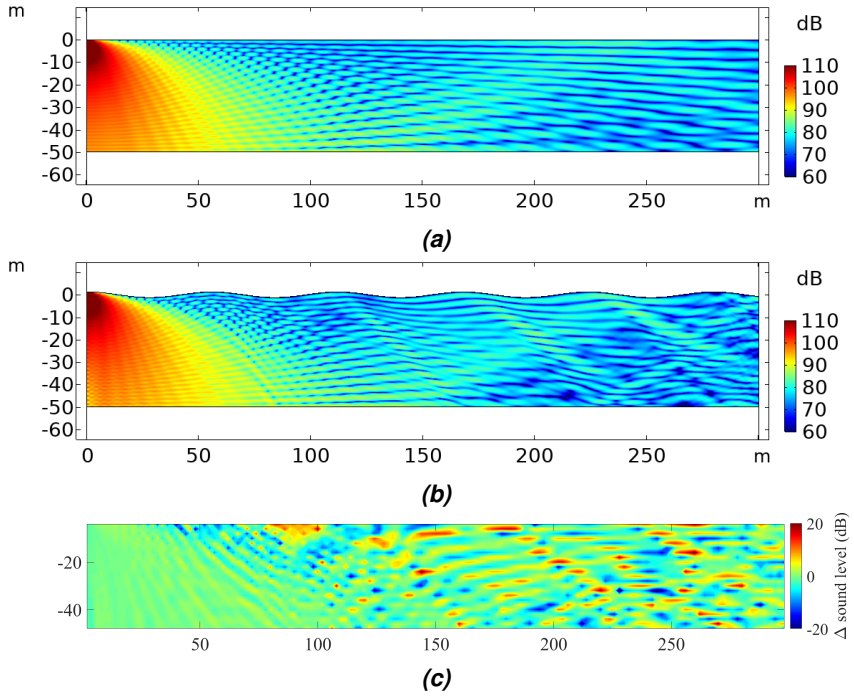

Figure 7: SL plot for shallow water: (a) SL_{flat}***; (b)*** SL_{crest}***; (c)*** $SL_{crest} - SL_{flat}$ ***at*** $d_{sw} = 50m$***,*** $\lambda_w = 56m$***,*** $d_s = 0.5m$***,*** $f_N = 500Hz$

The source beneath a wave trough increases the sound close to the surface, but the region in which this happens is smaller. Therefore, the average effect (shown in figure 6c) is a small reduction in the sound level compared with a flat free surface. Therefore, the average radiated noise level of a vessel travelling through a sea state is likely to be different due to this effect.

For the frequencies considered in this study, the results are very similar for source depths between 0.1 m and 1m as presented by Figure 5c where source is at 0.1m and 6a at 0.5m. This is most likely to the acoustic wavelength being longer than these distances.

3.3 Shallow water effects

Finally, the interaction between a wavy free surface and the seabed is considered for shallow water. Figure 7a and 7b presents the acoustic field in 50m-deep water under a flat and a wavy surface where source placed under wave crest. When the soft seabed is applied, reflections, scattering and adsorption change the propagation pattern resulting in constructive and destructive wave patterns. This also modifies the wavy surface's influence on Lloyd's mirror effect as can be seen in Figure 7c. This results in a more complex acoustic field, and this effect should be considered if conducting acoustic trials in a sea state either by using a larger hydrophone array or conducting more repeat runs.

4 CONCLUSIONS

This work has presented the results of numerical simulations of the Helmholtz equation to provide insights into the effect of a wavy free surface on acoustic propagation for a source close to the free surface. The results have been compared to those for a flat free surface. When the source is beneath a wave crest, the sound level close to the free surface is reduced, with the Lloyd's mirror effect effectively being amplified. For a source below a wave trough, the opposite occurs but to a lesser extent, resulting in a net reduction in the sound level close to the free surface. Future work will consider a much broader range of parameters combined with analytical modelling to develop robust models for understanding how a wavy surface modifies the propagation of underwater noise.

ACKNOWLEDGMENTS

The authors would like to thank Dr Reza Haqshenas for a number of useful discussions on approaches to the numerical modelling.

REFERENCES

1. ER Gerstein, JE Blue, and SE Forysthe. The acoustics of vessel collisions with marine mammals. In *Proceedings of OCEANS 2005 MTS/IEEE*, pages 1190–1197. IEEE, 2005.
2. T A Smith, A Grech La Rosa, and B Wood. Underwater radiated noise from small craft in shallow water: Effects of speed and running attitude. *Ocean Engineering*, 306:118040, 2024.
3. M Picciulin, E Armelloni, R Falkner, N Rako-Gospić, M Radulović, G Pleslić, S Muslim, H Mihanović, and T Gaggero. Characterization of the underwater noise produced by recreational and small fishing boats (¡ 14 m) in the shallow-water of the cres-lošinj natura 2000 sci. *Marine pollution bulletin*, 183:114050, 2022.
4. A Jones, J Sendt, A Duncan, P Clarke, and A Maggi. Modelling the acoustic reflection loss at the rough ocean surface. In *Proceedings of Acoustics 2009: Research to Consulting, Annual Conference of the Australian Acouscical Society*, pages 1–8. University of Adelaide, 2009.
5. A Jones, A Duncan, D Bartel, A Zinoviev, and A Maggi. Recent developments in modelling acoustic reflection loss at the rough ocean surface. In *Acoustics 2011: Breaking New Ground-Proceedings of the Annual Conference of the Australian Acousticial Society*, pages 1–8. The Australian Acoustical Society, 2011.
6. A P Rosenberg. A new rough surface parabolic equation program for computing low-frequency acoustic forward scattering from the ocean surface. *The Journal of the Acoustical Society of America*, 105(1):144–153, 1999.
7. Chris T Tindle and Grant B Deane. Shallow water sound propagation with surface waves. *The journal of the acoustical society of America*, 117(5):2783–2794, 2005.
8. E Larsson and L Abrahamsson. Helmholtz and parabolic equation solutions to a benchmark problem in ocean acoustics. *The Journal of the Acoustical Society of America*, 113(5):2446–2454, 2003.
9. Alexander O MacGillivray, S Bruce Martin, Michael A Ainslie, Joshua N Dolman, Zizheng Li, and Graham A Warner. Measuring vessel underwater radiated noise in shallow water. *The Journal of the Acoustical Society of America*, 153(3):1506–1524, 2023.
10. M A Ainslie and J G McColm. A simplified formula for viscous and chemical absorption in sea water. *The Journal of the Acoustical Society of America*, 103(3):1671–1672, 1998.